

The Formation of Uranus & Neptune: Challenges and Implications For Intermediate-Mass Exoplanets

Ravit Helled¹ and Peter Bodenheimer²

¹*Department of Geophysical, Atmospheric, and Planetary Sciences, Raymond and Beverly Sackler Faculty of Exact Sciences, Tel Aviv University, Tel Aviv, Israel*

²*UCO/Lick Observatory, Department of Astronomy and Astrophysics, University of California, Santa Cruz, CA 95064, USA*

ABSTRACT

In this paper we investigate the formation of Uranus and Neptune, according to the core-nucleated accretion model, considering formation locations ranging from 12 to 30 AU from the Sun, and with various disk solid-surface densities and core accretion rates. It is shown that in order to form Uranus-like and Neptune-like planets in terms of final mass *and* solid-to-gas ratio, very specific conditions are required. We also show that when recently proposed high solid accretion rates are assumed, along with solid surface densities about 10 times those in the minimum-mass solar nebula, the challenge in forming Uranus and Neptune at large radial distances is no longer the formation timescale, but is rather finding agreement with the final mass and composition of these planets. In fact, these conditions are more likely to lead to gas-giant planets. Scattering of planetesimals by the forming planetary core is found to be an important effect at the larger distances. Our study emphasizes how (even slightly) different conditions in the protoplanetary disk and the birth environment of the planetary embryos can lead to the formation of very different planets in terms of final masses and compositions (solid-to-gas ratios), which naturally explains the large diversity of intermediate-mass exoplanets.

1. Introduction

The increasing number of detected exoplanets with masses similar to those of Uranus and Neptune emphasizes the need to better understand the formation process of the planetary class consisting of planets with rock-ice cores of up to $\approx 15 M_{\oplus}$ and lower-mass hydrogen/helium envelopes, with a large range of solid-to-gas ratios. However, the formation mechanism for intermediate-mass planets is not well understood (e.g., Rogers et al. 2011),

and even within our own solar system there are many open questions regarding the formation of Uranus and Neptune.

Uranus and Neptune have masses of about 14.5 and 17 M_{\oplus} , and are located at 19.2 and 30 AU, respectively. Their exact compositions are not known (e.g., Helled et al. 2011), but they are likely to consist mainly of rock and ices with smaller mass fractions of hydrogen-helium atmospheres (see Fortney & Nettelmann 2010; Nettelmann et al. 2013 and references therein). The estimated solid-to-gas mass ratios of Uranus and Neptune range between 2.3 and 19 (Guillot 2005; Helled et al. 2011). Hereafter when we refer to the solid-to-gas ratio it should be clear that the solid component consists of all elements heavier than hydrogen and helium, and that in fact, their physical state can differ from a solid state, while the gas corresponds solely to hydrogen and helium. It is commonly assumed that Uranus and Neptune have formed by the core accretion scenario, in which solid core formation accompanied by slow gas accretion is followed by more rapid gas accretion (e.g., Pollack et al. 1996). During the initial phases of planet formation, the slow accretion of gas is controlled by the growth rate of its core. As a result, the solid accretion rate essentially determines the formation timescale of an intermediate-mass planet (see D’Angelo et al. 2011 for a review). The (standard) solid accretion rate is given by (Safronov 1969):

$$\dot{M}_{\text{core}} = \frac{dM_{\text{solid}}}{dt} = \pi R_{\text{capt}}^2 \sigma_s \Omega F_g, \quad (1)$$

where πR_{capt}^2 is the capture cross section for planetesimals, Ω is the orbital frequency, σ_s is the solid surface density in the disk, and F_g is the gravitational enhancement factor. As can be seen from Equation (1), the core accretion rate decreases with increasing radial distance, and as a result, the core formation timescale can be extremely long at radial distances larger than ~ 10 AU. Using the model of the minimum mass solar nebula (MMSN, see Weidenschilling 1977 for details), the formation timescales for Uranus and Neptune exceed 10^9 years (Safronov 1969). This estimate has introduced the *formation timescale problem of Uranus and Neptune*.

A detailed investigation of the formation of Uranus has been presented in Pollack et al. (1996). The authors have considered *in situ* formation and have shown that for σ_s about twice that of the MMSN the approximate core mass and envelope mass of Uranus are reached in about 16 Myr. The timescale is considerably shorter than that of Safronov primarily because of the use of improved (and much higher) values for F_g . The core accretion rate, however, depends not only on σ_s and F_g but also on the sizes of the accreted planetesimals. Smaller planetesimals can be accreted more easily, and it was shown by Pollack et al. (1996) that when planetesimals are assumed to have sizes of 1 km (instead of the standard 100 km) the formation timescale of Uranus decreases to ≈ 2 Myr. This timescale is within

the estimated range of lifetimes of gaseous protoplanetary disks but has been considered unrealistically short because of the use of a simplified core accretion rate in the model. Clearly, the formation timescale for Neptune under similar assumptions would be significantly longer. Due to the long accretion times at large radial distances, Uranus and Neptune are often referred to as “failed giant planets”, because their formation process was too slow to reach runaway gas accretion before the disk gas had dissipated.

Goldreich et al. (2004) discuss in detail the problem of the accumulation of solid particles, particularly at large distances from the central star. Without considering the effects of the gas, they suggest that to form Uranus- or Neptune-like planets *in situ*, one requires, first, relatively small planetesimals, < 1 km in radius, and second, a value of σ_s a few times that of the MMSN. In fact, they conclude that in order to form the planets within the lifetime of the gas disk, particles of only a few cm in size are needed. The small particles would be generated by collisions between the km-size objects. Numerous collisions among the small particles strongly damp the particle random velocities, resulting in a very cold disk. However, Levison & Morbidelli (2007), on the basis of N-body simulations, point out that this model is oversimplified and relies on numerous assumptions. They suggest that the main difficulty is the assumption that the surface density of the disk particles remains smooth and uniform. In fact the simulations show that the formation of rings and gaps actually dominates the dynamics.

The idea that the solar system was originally much more compact and that Uranus and Neptune were formed at smaller radial distances has been considered by a number of authors (e.g., Thommes et al. 1999; Tsiganis et al. 2005). The planets must arrive at their present locations post-formation, by gravitational scattering or by migration induced by a disk of planetesimals. The success of the “Nice Model” to explain many of the observed properties of the solar system led Dodson-Robinson & Bodenheimer (2010) to investigate the formation of Uranus and Neptune at radial distances of 12 and 15 AU, as suggested by that model. They adopted a disk model which accounts for disk evolution and disk chemistry (Dodson-Robinson et al. 2009), giving values of σ_s at those distances an order of magnitude higher than in the MMSN. The planet-formation calculation was similar to that of Pollack et al. (1996). It was found that the formation timescales of both Uranus and Neptune fell in the range 4–6 Myr, and that in some cases the solid-to-gas ratio was similar to those in the present planets. In addition, the results are consistent with the observed carbon enhancement in the atmospheres of these planets. It was therefore concluded that, indeed, Uranus and Neptune could have formed at smaller radial distances as implied by the Nice model. There are, however, unsolved issues with this formation scenario— for example, there is no way to distinguish Uranus from Neptune, and more importantly, there must be a

cutoff of both solid and gas accretion when the planets reach their current masses; otherwise the model predicts that they would continue to accrete to higher mass.

While the scenario in which Uranus and Neptune form at smaller radial distances is feasible and somewhat promising, there is no evidence for ruling out the possibility that these planets, and in particular extrasolar planets, could have formed at larger distances. Recent studies on the accretion rate of solids have provided new estimates for the rates in which solids are accreted to a planetary embryo in the core accretion paradigm (Rafikov 2011; Lambrechts & Johansen 2012). These studies suggest that the solid accretion rates can be significantly higher than previous estimates. With these high accretion rates the core formation timescale at large radial distances is significantly reduced. Although *in situ* formation of Neptune is considered unlikely (see below), *in situ* formation of Uranus as well as formation of extrasolar giant planets, or Neptune-sized planets, by core accretion at large radial distances might be feasible.

The aim of this paper is to re-investigate the formation of Uranus and Neptune (as representatives of intermediate-mass planets) and, in particular, to investigate the consequences of employing the high accretion rates mentioned in the previous paragraph. We account for various accretion rates, orbital locations, and disk properties. We employ a full core accretion–gas capture model. As we discuss below, formation of planets at 20 and 30 AU is, in principle, feasible, although their characteristics may not be those of Uranus and Neptune. We also suggest that a major challenge in forming Uranus and Neptune is to derive the correct final masses and the solid-to-gas ratios. However, the sensitivity of the properties of the forming planets to the assumed parameters provides a natural explanation for the diversity of extrasolar planets in the Uranus/Neptune mass regime.

2. The Formation Model and Its Parameters

To model the formation of the planets we use a standard core accretion model (e.g., Dodson-Robinson & Bodenheimer 2010; Lissauer et al. 2009), which combines a given core accretion rate with a detailed model of the structure of the gaseous envelope and for the interaction of incoming planetesimals with this envelope. The planetary formation calculation in core accretion theory usually begins with a small seed body surrounded by a swarm of planetesimals. Clearly, the formation of the initial core, even if small in mass, is not instant, and in some cases the formation time of the seed core can even be comparable to the planetary formation timescale. As a result, the formation timescales derived from most of our simulations, especially when considering large radial distances and/or low solid-surface

densities, should be taken as lower bounds. In the calculations presented here, the initial core mass is about $1 M_{\oplus}$, at which point a low-mass gaseous envelope has been accreted. These planetary embryos are assumed to form at given radial distances, and migration during the formation process is neglected. In some of the cases we do account for disk evolution, by gradually reducing the gas (and therefore also the small-dust) surface density with time. The planetesimals are assumed to be of a single size, which is a free parameter in the model. As discussed below, the planetesimal's size has some impact on the core accretion rates, but other parameters are found to be more important.

The structure of the gaseous envelope is calculated according to the standard spherically symmetric equations of stellar structure. The radiative opacities for the dust in the envelope are assumed to be reduced by approximately a factor 50 relative to standard interstellar dust opacities (e.g. Pollack et al. 1994). This reduction roughly accounts for the settling and coagulation of dust grains in the envelope (Movshovitz et al. 2010). The energy source in the envelope is provided primarily by the accretion of planetesimals, although gravitational contraction is also included. The gas accretion rate into the envelope is determined by the requirement that the outer radius of the planet (R_{pl}) match the modified accretion radius (Lissauer et al. 2009): $R_{\text{pl}}^{-1} = R_B^{-1} + 4R_H^{-1}$ where R_H is the Hill radius (see below) and $R_B = GM_{\text{pl}}/c_s^2$, the Bondi radius. Here M_{pl} is the total mass of the planet, and c_s is the sound speed in the disk.

2.1. Core Accretion Rates

The formation of the planet is essentially determined by the growth rate of the core. However, the growth rates for solid cores in the solar nebula are unknown, and must be inferred from models. Not surprisingly, the estimates for the core accretion rates have a large range, which can lead to rather different outcomes in terms of planetary formation. In order to investigate the sensitivity of the planetary formation to the assumed core accretion rate we consider three different accretion rates. The first corresponds to a dynamically cold planetesimal disk, providing high accretion rates, and is given by (Rafikov 2011):

$$\begin{aligned}\dot{M}_{\text{core}} &\approx 6.47\Omega p^{1/2}\sigma_s R_H^2 \\ &\approx 8.5 \times 10^{-4}\sigma_s M_{\text{core}}^{2/3}\end{aligned}\tag{2}$$

where M_{core} is the core mass, Ω is the orbital frequency, $p = R_{\text{core}}/R_H$, and $R_H = a(M_{\text{pl}}/(3M_{\odot}))^{1/3}$, the Hill radius, where a is the distance of the planet from the star. The second expression applies if $M_{\text{pl}} \approx M_{\text{core}}$ and under our standard assumption that the core is a sphere of constant density $\rho_{\text{core}} = 2 \text{ g cm}^{-3}$. This accretion rate can be taken as the maximum accretion

rate of solids according to Rafikov (2011). It should be noted that in this model the sizes of planetesimals are small, since large planetesimals are assumed to fragment into small pieces that are later affected by gas drag leading to the state of a dynamically cold planetesimal disk. Therefore, when this accretion rate is considered, the calculation is more consistent when the planetesimals are assumed to be small ($\ll 100$ km).

An alternative accretion rate was recently presented by Lambrechts & Johansen (2012) who find that accretion of pebbles (cm-sized particles) within the Hill radius is given by,

$$\dot{M}_{\text{core}} = 2R_H\sigma_s v_H, \quad (3)$$

where v_H is the relative velocity between the pebbles and the core, given by $v_H = \Omega R_H$. This expression applies when the core mass is higher than the transition mass (their Eq. 33)

$$M_t \approx 3 \times 10^{-3} (\Delta/0.05)^3 (a/5\text{AU})^{0.75} M_{\oplus} \quad (4)$$

where $\Delta = \Delta u_{\phi}/c_s$ represents the difference between the mean orbital gas flow and a pure Keplerian orbit (c_s is the disk sound velocity). At 15 AU $M_t \approx 0.055 M_{\oplus}$; thus this accretion rate is valid for all computations reported here. These accretion rates are higher by about one order of magnitude than the maximum accretion rates derived from Equation (2). In our work, we will set the high accretion rate to the one given by Equation (2) unless differently stated, and refer to it as $[\text{dM}/\text{dt}]_{\text{HIGH}}$.

Finally, the lower-bound accretion rate used in our model is the one derived for the "transition case" (Rafikov 2011) in which

$$\dot{M}_{\text{core}} \sim (6 - 10)pR_H\sigma_s v_H, \quad (5)$$

where $p \ll 1$. This rate refers to a "warm" planetesimal disk, with planetesimal random velocity dispersion s_p on the borderline between intermediate and high values ($s_p \approx \Omega R_H$). In the actual simulations we set the numerical coefficient equal to 2π . The rate is similar to the one used by Dodson-Robinson & Bodenheimer (2010) and is slightly lower than the accretion rates used by Pollack et al. (1996). Therefore, the rate derived from Equation (5) can be considered as the low (or standard) core accretion rate; we refer to it as $[\text{dM}/\text{dt}]_{\text{LOW}}$. Even lower rates are of course possible.

It should be noted, however, that core accretion rates are hard to estimate, and therefore the uncertainty in this quantity is rather large. As previously mentioned, detailed N-body simulations (Levison & Morbidelli 2007) suggest that the collisional damping scenario, needed to produce a planetesimal disk with low velocity dispersion, could be unreliable. Further N-body simulations (Levison et al. 2010) show that the gravitational interactions

between the embryo and the planetesimals lead to the wholesale redistribution of material and to the opening of gaps near the embryos. If the region near the growing embryo is cleared of planetesimals before much growth can occur, the core accretion rate will decrease dramatically and will prevent the formation of a giant and/or intermediate mass planet. Nevertheless, the possibility of a high solid accretion rate cannot be excluded. Various authors suggest that high core accretion rates can be maintained also over long timescales due to fragmentation, even at large radial distance (Goldreich et al. 2004; Rafikov 2011 and references therein). In view of the uncertainties, we take the approach of selecting representative accretion rates, which cover a rather wide range. Thus we can quantify the effect of the assumed core accretion rate (as well as other model assumptions) on the planetary growth.

2.2. Formation Locations

There is no simple way to constrain the original radial distances at which planets form. This is due to the fact that planets are likely to change their positions due to interactions with the disk (e.g., Kley & Nelson 2012) or with other planets (Thommes et al. 1999). Because of the location of the methane condensation front in the primitive solar nebula (Dodson-Robinson et al. 2009), Uranus and Neptune most probably formed beyond the orbit of Saturn, but whether they formed at the distances of ~ 12 -20 AU, as suggested by the Nice model, is yet to be determined. Formation of Neptune *in situ* at 30 AU is generally considered unlikely, and Malhotra (1995) and Hahn & Malhotra (1999) have shown that many properties of the Oort cloud and the Kuiper belt can be explained by the outward migration of Neptune, driven by a planetesimal disk. Nevertheless we present one test calculation involving formation at that distance. For our main results, we consider three formation locations of the planets: 12, 15 and 20 AU, radial distances that are predicted by and are consistent with the formation of Uranus and Neptune in the Nice Model. It should be noted, however, that within the framework of that model other orbital locations are possible as long as a separation of at least 2 AU between Uranus and Neptune is considered.

2.3. Solid Surface Densities

A critical unknown property in planet formation models is σ_s , the solid surface density in the disk. This parameter is important because it determines how much material is available for the formation of a core at the location where the planet is formed. In this work we

consider various possibilities for the solid-surface density. In most of the cases we consider, the lower bound for σ_s is similar to the one derived from the MMSM model (Weidenschilling 1977). The upper bound is typically about one order of magnitude higher than the MMSN model and is consistent with the solid surface densities derived by the disk model of Dodson-Robinson et al. (2009), in which condensation of various species of ices as well as disk evolution are included. Other solid-surface densities are considered as well. The σ_s that are used at various radial distances are listed in Table 1.

2.4. Planetesimal Sizes and Enhanced Planetesimal Capture Cross Section

As already discussed in Pollack et al. (1996), the planetary formation timescale decreases significantly when the accreted solids are small. Similarly to other disk properties, the sizes of planetesimals in the Solar Nebula are unknown, and in fact, they are likely to vary with radial distance and time. In addition, the planetesimals are expected to have a distribution of sizes. However, for simplicity, we consider single sizes for planetesimals. To investigate the effect of the planetesimal size on the planetary growth, we consider both small (1 km) and large (100 km) planetesimals. However the accretion rates given by Equations (2) and (3) imply that planetesimal sizes are smaller than 1 km. Therefore we have run one test with 50 meter planetesimals to investigate the effect of decreasing the size. Our experiments with a range of over three orders of magnitude in planetesimal size make it clear what the effect would be if even smaller sizes were taken, as discussed below.

The accretion rates defined by Equations (2) and (5) depend on the core radius R_{core} (note that Equation (3) does not depend on this quantity.) If the forming planet consists of a heavy-element core plus even a small amount of gas bound in an envelope, the capture rate of planetesimals is enhanced by the effects of gas drag and ablation as the accreting objects pass through the envelope. We account for the enhancement of the accretion rate by replacing R_{core} by R_{capt} , the effective capture radius. This quantity is determined at every time step by integration of the orbits of planetesimals as they approach the planet at various impact parameters and pass through the envelope. The details of how the procedure works are described in Pollack et al. (1996) based on earlier work by Podolak et al. (1988). The capture radius increases noticeably as the assumed planetesimal size decreases, and even for 100 km planetesimals, the ratio $R_{\text{capt}}/R_{\text{core}}$ can be a factor 10 if the envelope is sufficiently massive. This enhancement effect is included in most of the calculations reported here.

2.5. Planetesimal Ejection

Planetesimals are not only accreted by the growing planet but can also be ejected from the planet’s feeding zone. The effect of planetesimal ejection is more profound at large radial distances and is taken into account in our model. Following Ida & Lin (2004) the planetesimal ejection rate is calculated according to

$$f_{\text{cap}} = \frac{\text{accretion rate}}{\text{ejection rate}} = \left(\frac{2GM_{\odot}/a}{GM_{\text{core}}/R_{\text{core}}} \right)^2 \quad (6)$$

where M_{\odot} and M_{core} are the masses of the Sun and planetary core, respectively (in this case, R_{core} is the actual core radius, not an enhanced capture radius). The probability that a planetesimal will be scattered, rather than accreted, is then $1/(f_{\text{cap}} + 1)$. As Dodson-Robinson & Bodenheimer (2010) show, this probability approaches unity when $M_{\text{core}} \approx 10 M_{\oplus}$ and $a > 15$ AU. Thus it is an important factor in limiting the final mass of the planet. In fact the use of Equation (6) gives a lower bound on the actual scattering rate, as it takes into account only very close encounters and scatterings directly to unbound states. Future work should take scattering into account in a more detailed way.

2.6. Available Formation Timescale

The available time for forming a giant (or an *icy*) planet is typically taken to be the lifetime of the protoplanetary (gaseous) disk. At this point the gas disk dissipates and the planetary growth is terminated, at least, in terms of the gaseous component. The lifetimes of protoplanetary disks are derived from observations and are of the order of several million years. The median disk lifetime was found to be 3 Myr, a value we adopt in our model. However, some disks can survive on much longer timescales and can exist even up to 10 Myr (Hillenbrand 2008). In addition, the lifetime of gas in planetary disks can be longer than that of the dust, which can provide additional time for gas accretion. As a result, in some cases in which the planetary growth is limited by the disk’s lifetime, we allow the longer formation timescale and investigate the sensitivity of the formation model to the assumed available formation timescale. As we present below in several cases, the timing on which the gas disappears has a major impact on the final mass of the planets, and it can determine whether the planet will become a gas giant or not.

2.7. Solid-to-Gas Ratio

In addition to the final mass of the planets, which should be the same as the masses of Uranus and Neptune, formation models should also be able to lead to the correct solid-to-gas ratios within the planets. Although there is a fairly large uncertainty in the compositions of Uranus and Neptune (e.g., Fortney & Nettelmann 2010), there are several constraints on the fraction of hydrogen and helium which they can contain. As discussed in Guillot (2005, and references therein), under the assumption that the envelopes of the planets consist of ices and rocks, upper limits for the hydrogen and helium masses in Uranus and Neptune can be derived, and those masses are found to be $\approx 4.2 M_{\oplus}$ and $\approx 3.2 M_{\oplus}$, respectively. A lower bound of $\approx 0.5 M_{\oplus}$ for both Uranus and Neptune is inferred under the assumption that the outer envelope is pure hydrogen and helium.

3. Results

The parameters assumed for the various runs are listed in Table 1. Selected results are shown in Table 2, and the planet evolutions for most cases are plotted in Figures 1–7. The starting times for the plots in all cases are arbitrarily set at $\approx 2 \times 10^5$ yr, corresponding to the time required to build the initial core. However, the actual starting times will depend on a and σ_s . For example, Equation (8) of Rafikov (2011), which does not include the effects of scattering or enhancement of the capture radius by the presence of the envelope, would give starting times of 3×10^4 yr for Run 12UN2 (low a , high σ_s) to 4×10^6 yr for Run 30UN1 (high a , low σ_s). These time estimates are based on a solid accretion rate $[dM/dt]_{HIGH}$.

3.1. Formation at 20 AU

We first model the formation of a planet at radial distance of 20 AU, which corresponds to *in situ* formation for Uranus or to Neptune’s formation within the framework of the Nice model (Run 20UN1). Based on the MMSN model, at 20 AU $\sigma_s \approx 0.35 \text{ g cm}^{-2}$. The planetary core accretion rate is taken to be the maximum accretion rate $[dM/dt]_{HIGH}$ (Eq. 2), the enhanced planetesimal capture radius is taken into account with 1 km planetesimals, and planetesimal scattering is included. The planetary growth under these assumptions is shown in Figure 1. The red, blue, and black curves represent the mass of the gaseous envelope (mostly hydrogen and helium), core (heavy elements), and total planetary mass, respectively.

The upper panel shows the formation up to about 3 Myr. Under these conditions, the planetary growth is slow and the final planetary mass is $5 M_{\oplus}$, significantly smaller than the mass of Uranus. If the gas disk dissipates at 3 Myr, the forming planet will become a "mini-Neptune" with $M_{\text{core}} = 3.6 M_{\oplus}$ and $M_{\text{env}} = 1.4 M_{\oplus}$. However, if the disk lifetime is longer the planet can continue to grow. We then continue the formation to a longer timescale (see middle panel). As can be seen from the figure, at 8 Myr the planet can reach a mass exceeding $60 M_{\oplus}$. Clearly, in this case the lifetime of the disk plays a crucial role in the formation process. The calculation illustrates the point that even with $M_{\text{core}} < 4 M_{\oplus}$ the planet can reach crossover mass ($M_{\text{core}} = M_{\text{env}}$), given enough time. Crossover is actually obtained at 5.14 Myr at $M_{\text{core}} = 3.84 M_{\oplus}$.

Finally, we search for the timescale for the formation of a planet with Uranus's mass under these conditions. The result is shown in the bottom panel of the figure. To reach the mass of Uranus the gas disk has to dissipate at ≈ 7 Myr, and at ≈ 7.3 Myr in order to form a planet with Neptune's mass. It should be noted, however, that the final composition of the planets, assuming gas dissipation at about 7 Myr, is significantly different from that of Uranus/Neptune. The heavy element mass is only $5 M_{\oplus}$, while the rest is gas. Therefore, the forming planets will become something that is more like a "Mini-Saturn" rather than a Uranus/Neptune-like object.

As discussed in Dodson-Robinson & Bodenheimer (2010), the actual densities of the disk can be much higher than the ones derived from the MMSN model. In fact, the disk model of Dodson-Robinson et al. (2009) suggests that in the outer region of the disk, the solid surface densities are higher by a factor of 10. We therefore repeat the calculation at 20 AU (Run 20 UN2) but this time assume $\sigma_s = 3.5 \text{ g cm}^{-2}$ as derived by their disk model. Other parameters and assumptions are the same as in the run with $\sigma_s = 0.35 \text{ g cm}^{-2}$. The results are shown in the top panel of Figure 2. In that case the core accretion rate is higher which leads to a rapid growth. After only 0.55 Myr crossover mass is reached, at $16 M_{\oplus}$, and the planet can grow rapidly in mass. The simulation is stopped when the planet has reached $38 M_{\oplus}$ but gas accretion is expected to continue. We can conclude that the combination of high core accretion rates with relatively solid-rich disks leads to the formation of giant gaseous planets within relatively short timescales. Note, however, that M_{core} levels out at about $16 M_{\oplus}$. The isolation mass, which gives approximately the amount of solid material in the feeding zone of the planet, is given by $M_{\text{iso}} = 1.56 \times 10^{25} (a^2 \sigma_s)^{3/2} \text{ g}$, where a is given in AU and σ_s in cgs units. In this case $M_{\text{iso}} \approx 136 M_{\oplus}$, but scattering, particularly at high core mass, removes a large fraction of that material. In fact at the end of the simulation, practically all solid material available to the planet has either been accreted or scattered.

We next model (Run 20UN3) the formation at 20 AU with $\sigma_s = 0.7 \text{ g cm}^{-2}$, which is

about twice the MMSN value. The core accretion rate is set to its maximum value, and both the effect of planetesimal scattering and cross section enhancement due to the planetary envelope are *not* included. The results are shown in the middle panel of Figure 2. In that case, a planet similar to Neptune can be formed within 1.3 Myr. At that point the core mass is $\sim 15 M_{\oplus}$ with an envelope of $4 M_{\oplus}$. If the simulation continues to longer times more gas is accreted and the forming planet will become a gas giant planet. Under these conditions, in order to form a Neptune-like planet the gas has to dissipate relatively early. Note, however, that the planetary growth is expected to be slower and the final heavy-element mass is expected to be smaller when planetesimal scattering is included. Finally, we model, in Run 20UN4, the planetary growth at 20 AU, $\sigma_s = 1.7 \text{ g cm}^{-2}$ but this time with the transitional core accretion rate $[dM/dt]_{LOW}$ (Eq. 5). The results are presented in the bottom panel of Figure 2. Even with the low accretion rate it is found that a planet of similar mass to that of Uranus can be formed within less than 2 Myr; however, the gaseous mass is significantly higher than that of Uranus.

Clearly, the properties of the planet can change significantly even due to changes in the solid-surface density alone. We can also conclude that the high accretion rates can now allow for *in situ* formation at 20 AU, even when the MMSN solid surface densities are used. However in that case, with very low surface density, the conclusion is marginal. First, as mentioned, the time required to reach Uranus mass is 7 Myr, which is beyond the lifetime of most gas disks. Second, to allow the use of the maximum accretion rate, the embryo has to grow big enough to excite the planetesimal velocities so that they collide, fragment, and produce the required small particles. Based on the work of Rafikov (2003, 2004), at 20 AU and in the MMSN, the required embryo mass is of order 10^{24} g , and the time to build that embryo is very roughly estimated at 10^6 to 10^7 yr . Therefore a detailed numerical simulation of the planetesimal dynamics, including fragmentation, is required to determine whether the use of the high accretion rate is justified in this particular case. At smaller distances from the Sun, or with higher values of σ_s , the corresponding time is considerably shorter.

3.2. Formation at 15 AU

In this section we investigate the formation of a planet at 15 AU. First (Run 15UN1), we consider $\sigma_s = 0.55 \text{ g cm}^{-2}$, close to the value in the MMSN. The core accretion rate is set to $[dM/dt]_{HIGH}$, scattering of planetesimals is included, and envelope enhancement is included. The results are shown in the top panel of Figure 3. With this low surface density the planetary growth is slow and at $\sim 2.5 \text{ Myr}$ the planet has a core mass of $3.6 M_{\oplus}$ and an envelope mass of $0.8 M_{\oplus}$. At 9.7 Myr crossover mass is still not reached, and the planet has

a core mass of about $4 M_{\oplus}$ and an envelope of $3.1 M_{\oplus}$. Clearly, under these assumptions it is not possible to form a Neptune/Uranus mass planet. It should be noted, however, that at the point the simulation stops, the gas accretion rate is about $0.3 M_{\oplus}/\text{Myr}$, therefore a slightly higher solid surface density and/or longer disk lifetime would probably lead to the formation of a gaseous planet.

We next model the planetary formation at 15 AU with $\sigma_s = 5.5 \text{ cm}^{-2}$ (Run 15UN2). Other assumptions are the same as in the previous case. It is found that the crossover mass is reached already after $\approx 6 \times 10^5$ years when the core and envelope masses are $18.9 M_{\oplus}$. The results for this case are shown in the bottom panel of Figure 3. Clearly, this combination of parameters is more preferable for giant planet formation than formation of intermediate-mass planets.

The use of $[dM/dt]_{\text{HIGH}}$ implies that small planetesimals, less than 100 meters in size, dominate the accretion (Rafikov 2004). Our calculations with 1 km planetesimals are not entirely consistent; therefore we run a calculation with planetesimal size 50 meters and otherwise with the parameters of Run 15UN1. In our calculation the only effect of decreasing the planetesimal size is to increase the enhancement of the cross section for planetesimal capture. Thus the phase during which core accretion dominates is shortened; this phase is short in any case. Once the core mass approaches its limiting value, and envelope accretion is the dominant process, the effect of the smaller planetesimals is very small. In Run 15UN3, the limiting core mass is approached only 2.2×10^5 years after the start, while in Run 15UN1 the corresponding time is 3.25×10^5 years. In Run 15UN3 at 2.5 Myr, the core mass is $3.62 M_{\oplus}$ and the envelope mass is $0.85 M_{\oplus}$, practically the same as in Run 15UN1. The calculation in 15UN3 is run to 9.7 Myr, as in Run 15UN1, and at that time the core mass is $4.03 M_{\oplus}$ and the envelope mass is $3.65 M_{\oplus}$. These results give the same conclusion as in Run 15UN1: with these assumptions it is not possible to produce a Uranus or Neptune mass planet in a reasonable time.

3.3. Formation at 12 AU

We next model the formation of a planet at 12 AU, the minimum radial distance for the formation of Uranus/Neptune as suggested by the Nice model. At 12 AU the solid surface density is relatively high, providing preferable conditions for planet formation.

First (Run 12UN1), we consider a solid surface density of $\sigma_s = 0.75 \text{ g cm}^{-2}$, which is approximately that of the MMSN at that radial distance, and assume the high solid accretion rate (Eq. 2). As in previous cases, the enhancement of the capture rate is included, with 1

km planetesimals. The results are shown in the top panel of Figure 4. The planetary growth is somewhat similar to that derived for the low-density case at 20 AU. The core mass reaches $\approx 3.5 M_{\oplus}$ relatively fast and then levels off, while the envelope mass reaches $0.65 M_{\oplus}$ at 2.5 Myr. Clearly, under these conditions it is not possible to form a planet which resembles Uranus/Neptune. In order to demonstrate whether it is possible to form a Uranus/Neptune-like planet we continue the simulation up to 10 Myr. At that time we obtain $M_{\text{core}} = 3.8 M_{\oplus}$ and $M_{\text{env}} = 2.2 M_{\oplus}$. We can therefore conclude that under such conditions it is not possible to form a planet of the order of $15 M_{\oplus}$; instead a Super-Earth or Mini-Neptune planet is formed. Comparing Runs 20UN1 and 12UN1, both runs having low surface densities, the former case develops a somewhat higher core mass, because more solid material is available in the disk at the larger distance. The envelope accretion rate is strongly dependent on the core mass (Pollack et al. 1996), so 20UN1 is able to reach crossover in < 10 Myr, while 12UN1 is not.

We next consider planet formation with $\sigma_s = 7.5 \text{ g cm}^{-2}$ which corresponds to ≈ 10 times MMSN (Run 12UN2). Other assumptions are the same as in the previous case. The results are shown in the lower panel of Figure 4. Under these conditions the growth of the planet is rapid, and at 0.52 Myr it reaches the crossover mass of $21 M_{\oplus}$ which leads to rapid gas accretion. The simulation was terminated at 0.56 Myr with a total mass of $48 M_{\oplus}$ and an envelope mass of $\approx 26 M_{\oplus}$. If the disk lifetime under these conditions is of the order of several Myr, a gaseous planet is expected to form. This simulation is similar to the one at 15 AU with the high solid-surface density. In both cases, a giant planet can be formed quickly. By the end of both runs most of the planetesimals in the feeding zone have either been accreted onto the core or scattered. However, closer to the Sun, a larger fraction of the planetesimals can be accreted; while at 12 AU $f_{\text{cap}} = 0.18$ at the end of the simulation, at 15 AU, $f_{\text{cap}} = 0.13$. Thus M_{core} at crossover is somewhat smaller at 15 AU (18.9 vs. $21 M_{\oplus}$), and because of the lower surface density at 15 AU, the time to reach crossover is somewhat longer (6.2×10^5 vs. 5.2×10^5 yr.)

We next consider (Run 12UN3) the high solid surface density case (i.e., $\sigma_s = 7.5 \text{ g cm}^{-2}$) but this time using the “transition” accretion rate $[dM/dt]_{\text{LOW}}$ (Eq. 5). Other parameters are the same as in the previous case. The results are shown in the top panel of Figure 5. Even under these conditions the planetary growth is fairly rapid and after about 0.9 Myr the planet has reached a total mass of $\approx 45 M_{\oplus}$ with an envelope mass of $24 M_{\oplus}$. This case is very similar to the previous case using the maximum accretion rate, with the main difference being the timescale to reach the crossover mass. Nevertheless, due to the high solid surface density, a giant planet can be formed within the lifetime of most protoplanetary disks. In these cases, the challenge is to form planets with final masses similar to those of Uranus

and Neptune. If Uranus/Neptune indeed formed at 12 and/or 15 AU, they can provide important constraints on σ_s and the accretion rates at these locations, since according to our simulations, the growing planets can become gaseous planets fairly easily.

This case was recalculated with a planetesimal size of 100 km rather than 1 km, again using $[dM/dt]_{LOW}$ (not plotted or listed). The end result was practically the same, namely, the onset of rapid gas accretion, with a crossover mass of about $21 M_{\oplus}$. The time to reach crossover, however was twice as long, 1.8 Myr instead of 0.9 Myr, as a result of the reduced enhancement of the planetesimal capture cross section with the larger planetesimals.

The case discussed in the previous paragraph is somewhat similar to a calculation done by Dodson-Robinson & Bodenheimer (2010), who considered planet formation at 12 AU with $\sigma_s = 8.4 \text{ g cm}^{-2}$. In their calculation, planetesimal scattering was included but the core accretion rate was a factor 2 lower than $[dM/dt]_{LOW}$. Their result shows that Uranus mass is reached at 4 Myr with $M_{\text{core}} = 13.5 M_{\oplus}$ and $M_{\text{env}} = 1.0 M_{\oplus}$. Neptune mass is reached at 4.2 Myr with $M_{\text{core}} = 15 M_{\oplus}$ and $M_{\text{env}} = 2 M_{\oplus}$. However, if the disk does not dissipate until later times, accretion can continue up to much higher masses. We have redone this simulation with the same parameters but with an improved version of the formation code. We take a planetesimal size of 100 km to be consistent with their assumptions. Our results show that Uranus mass is reached at 1.76 Myr with $M_{\text{core}} = 13.9 M_{\oplus}$ and $M_{\text{env}} = 0.6 M_{\oplus}$. Neptune mass is reached at 1.89 Myr with $M_{\text{core}} = 16 M_{\oplus}$ and $M_{\text{env}} = 1 M_{\oplus}$. Again, accretion continues to higher masses. Our times are about a factor 2 shorter than those of Dodson-Robinson & Bodenheimer (2010), mainly because the envelope enhancement of the planetesimal capture cross section is more accurately calculated in our case and turns out to be higher.

Finally (Run 12UN4), we model the formation of a planet at 12 AU, with the transitional accretion rate but with lower σ_s than in Run 12UN3. The results are shown in the bottom panel of Figure 5. Although the formation timescale is longer compared to that in Run 12UN3, it is found that crossover mass can be reached within ≈ 2.5 Myr. The value of the crossover mass is, however, almost a factor 2 lower than in Run 12UN3. At this point the planetary mass is over $20 M_{\oplus}$, and the solid-to-gas ratio is close to 1.

3.4. The Effect of Planetesimal Scattering - A Test At 30 AU

The farthest formation location so far considered in this work is 20 AU, which is typically considered as an upper bound for Uranus and Neptune based on the Nice model. Formation at larger radial distances is however possible. Since the surface density decreases with radial

distance the formation process is somewhat less efficient and the forming planets are expected to have smaller masses. Nevertheless, with high core accretion rates, and with sufficiently high σ_s even at 30 AU planets could be formed, and even become gas giants. Our simulations, however, are limited to the case where σ_s is close to the value for the MMSN.

It should be noted, however, that our simulations start with solid cores of $\approx 1.3 M_\oplus$. At 30 AU, the timescale for forming such cores can be a few million years, which delays the formation process significantly. In addition, planetesimal scattering is more important for large radial distances. In this section we model planetary formation at 30 AU. In order to demonstrate the importance of planetesimal scattering and its crucial effect on the planetary growth, we compare two cases of planet formation at 30 AU (Runs 30UN1 and 30UN2), which differ solely by this assumption. The solid surface density is assumed to be low, 0.2 g cm^{-2} , and the high accretion rate $[dM/dt]_{HIGH}$ is used. The results are shown in Figure 6. The top panel presents the planetary growth when planetesimal scattering is included. It is found that after 3 Myr, a planet with a total mass of $\approx 5 M_\oplus$ is formed. The gaseous mass by the end of the simulation is $1.6 M_\oplus$. The planetary growth is somewhat similar to that in Run 20UN1, at 20 AU with the low σ_s (Figure 1). If the planet is allowed to grow on a longer timescale, crossover mass is expected to be reached before 10 Myr, leading to the formation of a giant or intermediate mass planet within 10 Myr. The total mass of heavy elements is, however, small, and therefore, regardless of the final mass of the planet, it is expected to be gas-dominated. The results for the planetary growth when planetesimal scattering is *not* considered (Run 30UN2) are shown in the bottom panel. In this case the planet can grow faster, and crossover is reached after ≈ 2.5 Myr with a higher solid mass than in Run 30UN1. In that case Uranus/Neptune-mass planets can be formed even at 30 AU. For the case without planetesimal scattering, even if we add the ≈ 4.4 Myr that are required to build the seed core, intermediate-mass and gas giant planets can be formed at 30 AU when disk lifetimes are of the order of 10 Myr. The solid-to-gas ratio by the end of the simulation is close to one. Clearly, planetesimal scattering plays a major role in planet formation models, when relatively large radial distances are considered, and it has a crucial effect on both the formation timescale and the final composition of the planets.

However, at a distance of 12 AU the effect is much less important. A comparison to Run 12UN1 was run without scattering (not plotted or listed). The run without scattering also did not reach crossover; at 7 Myr it reached $M_{\text{core}} = 5.05 M_\oplus$ and $M_{\text{env}} = 2.84 M_\oplus$, in comparison with $M_{\text{core}} = 3.7 M_\oplus$ and $M_{\text{env}} = 1.62 M_\oplus$ at the same time in Run 12UN1.

3.5. The Effect of the Planetesimal Size

Clearly, since small planetesimals are more affected by the gaseous envelope, the planetary growth is more efficient when small planetesimals are assumed. We next present two cases (Runs 20UN5 and 12UN5) in which the planetesimals are assumed to be relatively large, i.e. 100 km (see also Section 3.2, Run 15UN3). Results for the two runs with 100 km-sized planetesimals are shown in Figure 7. The top panel (Run 20UN5) corresponds to formation at 20 AU with the maximum accretion rate and $\sigma_s = 0.35 \text{ g cm}^{-2}$, i.e., similar to the case presented in Figure 1 but assuming 100 km-sized planetesimals instead of 1 km. By comparing the two cases it can be concluded that although the growth is slightly slower in Run 20UN5, the overall growth of planet after 3 Myr is very similar. At 3 Myr the core mass is found to be $3.57 M_\oplus$ and the envelope mass $1.6 M_\oplus$, compared to $M_{\text{core}} = 3.55 M_\oplus$ and $M_{\text{env}} = 1.43 M_\oplus$ in Run 20UN1 at the same time. The main difference between these two cases is that when larger planetesimals are used, it takes a somewhat longer time to build up the core during the earlier phases to the (scattering limited) mass of $\sim 3.5 M_\oplus$.

The bottom panel of Figure 7 illustrates Run 12UN5, at 12 AU with $\sigma_s = 3 \text{ g cm}^{-2}$, $[\text{dM}/\text{dt}]_{\text{LOW}}$, and 100 km planetesimals. This case should be compared with Run 12UN4 (bottom panel of Figure 5), which has the same parameters except for a planetesimal size of 1 km; crossover mass of $11.6 M_\oplus$ is reached after 2.3 Myr. With 100 km planetesimals, a Uranus-mass planet can be formed within about 3.3 Myr, with core mass $10.5 M_\oplus$ and envelope mass $4.0 M_\oplus$. After that point the gas accretion rate is significantly higher than the core accretion rate; as a result a planet with Neptune’s mass can be formed under these conditions after 3.6 Myr, with $M_{\text{core}} = 10.9 M_\oplus$ and $M_{\text{env}} = 6.1 M_\oplus$. The solid-to-gas ratio is too low compared with that of Neptune; however the case with the higher planetesimal size leads to a higher solid-to gas ratio at times around 3 Myr, since crossover mass is not reached by that time.

3.6. The Lambrechts–Johansen (LJ) Accretion Rate

The LJ rate (Eq. 3) is higher than $[\text{dM}/\text{dt}]_{\text{HIGH}}$ by roughly one order of magnitude, depending on the stage of evolution. The cases with high σ_s , which include Runs 20UN2, 15UN2, 12UN2, and 12UN3, all reach crossover mass in relatively short times. If these runs were to be redone with the LJ rate, they would simply reach crossover mass faster, with similar core masses; the core masses are determined by the amount of solid material available and by the effects of scattering, not by the accretion rate. On the other hand, the low σ_s cases, which include Runs 20UN1, 15UN1, 12UN1, 30UN1, and 20UN5, do not reach

crossover in 3 Myr, although they could over longer times. The core masses, which fall in the range 3–4 M_{\oplus} at 3 Myr, are limited by the isolation mass, which increases as $a^{3/4}$ in the MMSN, as reduced by the effects of scattering, which become more important at larger a . The gas accretion rates at these low core masses are slow, and are little affected by the core accretion rate, once the limiting core masses have been reached. Thus the use of a faster core accretion rate would simply speed up the time to approach the limiting core mass but would have little effect on the results at longer times.

A test calculation has been run at 20 AU and $\sigma_s = 0.35 \text{ g cm}^{-2}$, with the LJ rate. A core mass of 3.2 M_{\oplus} is reached after 5×10^4 years after the start, as compared with about 3×10^5 yr in the comparison run 20UN1 (top panel of Figure 1). The end result for the test case after 3 Myr is $M_{\text{core}} = 3.65 M_{\oplus}$ and $M_{\text{env}} = 2.13 M_{\oplus}$, while for Run 20UN1 the corresponding numbers are 3.59 and 1.72 M_{\oplus} , respectively. Thus the basic conclusions of this paper are only weakly affected by the choice of Equation (3) rather than Equation (2).

A problem may arise, however, in the use of the LJ theory. The time to reach the transition mass, Equation (4), can be quite long. In fact the LJ estimate of the time to reach this mass (their Eq. 42) exceeds 10^8 yr at 20 AU. Thus fast accretion by this mechanism requires, first, that a significant fraction of the solid material be in the form of “pebbles” (cm-size particles) close to the midplane, and second, that at least some planetesimals close to the transition mass (≈ 1000 km in size) must have formed early by some independent process (Lambrechts & Johansen 2012).

4. Conclusions

Understanding the formation of Uranus and Neptune is crucial for understanding the origin of our solar system, and in addition, the formation of intermediate-mass planets around other stars. Planets that are similar to Uranus and Neptune in terms of mass are likely to form by core accretion, i.e., from a growing solid core which accretes gas at a lower rate, although alternative mechanisms should not be excluded (Boss et al. 2002; Nayakshin 2011). If indeed formed by core accretion, such planets must form fast enough to ensure that gas is accreted onto the core, but at the same time slow enough, in order to remain small in mass and not become gas giant planets.

Our study shows that simulating the formation of Uranus and Neptune is not trivial, and that getting the correct masses and solid-to-gas ratio depends on the many (unknown) model parameters. Even small changes in the assumed parameters can lead to a very different planet. The core accretion rate and the disk’s properties such as solid-surface density and the

planetesimals’ properties (sizes, dynamics, etc.) play a major role in the formation process, and even small changes in these parameters can influence the final masses and compositions of the planets considerably.

We have used high accretion rates for the solids and have investigated their impact on the planet formation process. With these high accretion rates and with values of σ_s about 10 times those in the MMSN, the formation timescale problem for formation of Uranus or Neptune at 20 AU disappears. However, a new problem arises - the formation of the planets can be so efficient that instead of becoming failed giant planets, Uranus and Neptune would become giant planets, similar to Jupiter and Saturn. The situation becomes even worse with formation at smaller radial distance where the solid surface density is high. At radial distances such as 12 and 15 AU, the planets reach runaway gas accretion within a timescale which is shorter than the average lifetimes of protoplanetary disks, leading to the formation of gaseous giant planets.

However, if the values of σ_s appropriate for the MMSN are used, a different problem arises. Even with high core accretion rates, the resulting solid masses are too low compared with those of Uranus/Neptune, at all distances. Scattering of planetesimals is an important effect in this regard. Our results suggest that intermediate values of σ_s , perhaps combined with relatively low core accretion rates (e.g. Run 12UN5), are needed to satisfy the joint constraints provided by disk lifetimes, total masses, and solid-to-gas ratios.

It should be noted that the “true” core accretion rate to form Uranus and Neptune is not known and could be different from the values we consider here. Our work shows that even with a relatively low accretion rate, combined with a relatively high solid surface density σ_s , it is possible to form a giant planet in a relatively short time (Run 12UN3). However, different, but still reasonable choices for these parameters can produce quite different results; for example Run 12UN1 produces a planet of less than half the mass of Uranus after 10 Myr. Finding the right set of parameters that will lead to the formation of planets with the final masses of Uranus and Neptune is challenging, and getting the correct gas masses is even harder. In some cases the gas accretion rate becomes high enough and an increase in mass to the Uranus/Neptune mass range occurs, but the solid-to-gas ratio in the models is inconsistent with that of Uranus and Neptune (see Table 2). The cases we present simply demonstrate the sensitivity of the planetary formation to the assumed parameters, and while they do provide possible scenarios for the formation of Uranus and Neptune, they are certainly not unique. Clearly, the core accretion rate is a major uncertainty in planet formation models, and a better determination of this property (and its time evolution) will have a significant impact on simulations of planetary growth of both terrestrial and giant planets.

Our work suggests that under the right conditions, *in situ* formation for Uranus at 20 AU, or formation of Neptune at about the same distance, is possible. At 30 AU, our run with σ_s near the value for the MMSN and with planetesimal scattering, showed that a Neptune-mass planet was not formed. Although Rafikov (2011) shows that the use of the high accretion rate should result in evolution to rapid gas accretion out to 40–50 AU in a MMSN in 3 Myr, our result is different. The main reason is that planetesimal scattering limits the core mass to about $3.3 M_\oplus$, leading to a slow accretion rate for the envelope. However that result could change if a higher value of σ_s were taken.

In situ formation at relatively large radial distances seems to be possible for intermediate-mass planets in general. In addition, high solid surface density, which is expected in metal-rich environments, can lead to fast core formation, and therefore to the formation of giant planets instead of intermediate-mass planets. The latter provides a natural explanation to the correlation between stellar metallicity and the occurrence rate of gas giant planets. Nevertheless, we also find that giant planets can be formed in low-metallicity environments. As a result, giant planets around low-metallicity stars should not necessarily be associated with formation by gravitational instability. It is also concluded that the formation of Uranus/Neptune-mass planets is not always challenging in terms of the formation timescale but often, in terms of reducing the gas accretion in order to prevent the formation of gaseous planets.

Finally, while our work emphasizes once more the difficulty to simulate the formation of the solar-system planets very accurately, it provides a natural explanation for the diversity in planetary parameters in extrasolar planetary systems. Since planetary disks are expected to have different physical properties (e.g., surface densities, lifetimes) it is clear that the forming planets will have different growth histories, as well as different final masses and compositions.

Acknowledgments

P. B. was supported in part by a grant from the NASA program “Origins of Solar Systems”.

REFERENCES

- Boss, A. P., Wetherill, G. W. & Haghighipour, N. 2002. *Icarus*, 156, 291
- D'Angelo, G., Durisen, R. H. & Lissauer, J. J. 2011. In: *Exoplanets*, ed. S. Seager (Tucson: Univ. of Arizona Press), 319
- Dodson-Robinson, S. E. & Bodenheimer, P. 2010. *Icarus*, 207, 491
- Dodson-Robinson, S. E., Willacy, K., Bodenheimer, P., Turner, N. J., & Beichman, C. A. 2009. *Icarus*, 200, 672
- Fortney, J. J. & Nettelmann, N. 2010. *Space Sci. Rev.*, 152, 423
- Goldreich, P., Lithwick, Y. & Sari, R. 2004. *Annu. Rev. Astron. Astrophys.*, 42, 549
- Guillot, T. 2005. *Annu. Rev. Earth Planet. Sci.*, 33, 493
- Hahn, J. M. & Malhotra, R. 1999. *AJ*, 117, 3041
- Helled, R., Anderson, J. D., Podolak, M. & Schubert, G. 2011. *ApJ*, 726, 15
- Hillenbrand, L. 2008. *Phys. Script.*, 130, 014024.
- Ida, S. & Lin, D. N. C. 2004. *ApJ*, 604, 388
- Kley, W. & Nelson, R. 2012. *Annu. Rev. Astron. Astrophys.*, 50, 211
- Lambrechts, M. & Johansen, A. 2012. *A&A*, 544, A32
- Levison, H. F., Duncan, M. J. & Thommes, E. W. 2010, *AJ*, 139, 1297
- Levison, H. F. & Morbidelli, A. 2007, *Icarus*, 189, 196
- Lissauer, J. J., Hubickyj, O., D'Angelo, G. & Bodenheimer, P. 2009, *Icarus*, 199, 338
- Malhotra, R. 1995, *AJ*, 110, 420
- Movshovitz, N., Bodenheimer, P., Podolak, M. & Lissauer, J. J. 2010. *Icarus*, 209, 616
- Nayakshin, S. 2011. *MNRAS*, 416, 2974
- Nettelmann, N., Helled, R., Fortney, J. J. & Redmer, R. 2013. *Planet. Space Sci.*, 77, 143
- Podolak, M., Pollack, J. B. & Reynolds, R. T. 1988. *Icarus*, 73, 163

- Pollack, J. B., Hollenbach, D., Beckwith, S. et al. 1994. ApJ, 421, 613
- Pollack, J. B., Hubickyj, O., Bodenheimer, P. et al. 1996. Icarus, 124, 62.
- Rafikov, R. R. 2003. AJ, 125, 942
- Rafikov, R. R. 2004. AJ, 128, 1348
- Rafikov, R. R. 2011. ApJ, 727, 86
- Rogers, L. A., Bodenheimer, P., Lissauer, J. J. & Seager, S. 2011. ApJ, 738, 59
- Safronov, V. S. 1969. Evolution of the Protoplanetary Cloud and Formation of the Earth and Planets (Moscow: Nauka), in Russian. English translation: NASA-TTF-677, (Jerusalem: Israel Sci. Transl. 1972)
- Thommes, E. W., Duncan, M. J. & Levison, H. F. 1999. Nature, 402, 635
- Tsiganis, K., Gomes, R., Morbidelli A. & Levison, H. F. 2005. Nature, 435, 459
- Weidenschilling, S. J. 1977. Astrophys. Space Sci., 51, 153

RunName	Radial Distance (AU)	σ_s (g cm^{-2})	P-Size(km)	P-Scattering	$T_{\text{neb}}(K)$	ρ_{neb} (g cm^{-3})	\dot{M}_{core}
20UN1	20	0.35	1	YES	20	8×10^{-13}	eq. (2)
20UN2	20	3.5	1	YES	20	8×10^{-12}	eq. (2)
20UN3	20	0.7	1	NO	20	1.6×10^{-12}	eq. (2)
20UN4	20	1.7	1	YES	20	4×10^{-12}	eq. (5)
15UN1	15	0.55	1	YES	40	1.7×10^{-12}	eq. (2)
15UN2	15	5.5	1	YES	40	1.7×10^{-11}	eq. (2)
15UN3	15	0.55	0.05	YES	40	1.7×10^{-11}	eq. (2)
12UN1	12	0.75	1	YES	50	3×10^{-12}	eq. (2)
12UN2	12	7.5	1	YES	50	3×10^{-11}	eq. (2)
12UN3	12	7.5	1	YES	35	3×10^{-11}	eq. (5)
12UN4	12	3	1	YES	50	1.2×10^{-11}	eq. (5)
30UN1	30	0.2	1	YES	20	3×10^{-13}	eq. (2)
30UN2	30	0.2	1	NO	20	3×10^{-13}	eq. (2)
20UN5	20	0.35	100	YES	20	8×10^{-13}	eq. (2)
12UN5	12	3	100	YES	50	1.2×10^{-11}	eq. (5)

Table 1: The various cases considered in this work. σ_s is the solid surface density at a given radial distance, “P-Size” is the planetesimal size, “P-Scattering” indicates whether planetesimal scattering is included in the simulation, T_{neb} and ρ_{neb} are the temperature and density of the disk at the formation location of the planet and \dot{M}_{core} is the assumed core accretion rate.

RunName	$t_{\text{crossover}}$ Myr	$M_{\text{crossover}}$ M_{\oplus}	t_{end} Myr	$M_{\text{core,end}}$ M_{\oplus}	$M_{\text{env,end}}$ M_{\oplus}	$M_{\text{tot,end}}$ M_{\oplus}	$f_{\text{solid-to-gas}}$	$\dot{M}_{\text{core,end}}$ $M_{\oplus} \text{ yr}^{-1}$	$\dot{M}_{\text{env,end}}$ $M_{\oplus} \text{ yr}^{-1}$
20UN1	5.14	3.83	7.9	5.6	60	65.6	0.09	1.5×10^{-5}	1.9×10^{-4}
20UN2	0.54	15.8	0.59	16.2	20.3	36.5	0.8	3.0×10^{-5}	6.0×10^{-5}
20UN3	—	—	1.3	14.3	3.9	18.2	3.67	3.3×10^{-6}	8.8×10^{-6}
20UN4	—	—	1.67	9.8	4.8	14.6	2.04	2.0×10^{-6}	1.6×10^{-5}
15UN1	—	—	9.7	4.0	3.1	7.1	1.29	3.2×10^{-8}	3.0×10^{-7}
15UN2	0.62	18.9	0.63	19.4	26.2	45.6	0.74	3.3×10^{-5}	1.3×10^{-4}
15UN3	-	-	9.7	4.03	3.65	7.7	1.10	3.2×10^{-8}	4.0×10^{-7}
12UN1	—	—	10.0	3.8	2.2	6.0	1.73	2.3×10^{-8}	1×10^{-7}
12UN2	0.52	21.2	0.56	21.5	26.1	47.6	0.82	8.1×10^{-5}	4.2×10^{-4}
12UN3	0.89	20.8	0.90	21.0	23.9	44.9	0.88	5.5×10^{-5}	4.1×10^{-4}
12UN4	2.39	11.6	2.40	11.6	11.7	23.3	0.99	1.3×10^{-6}	5.4×10^{-6}
30UN1	—	—	3.1	3.3	1.6	4.9	2.06	1.9×10^{-7}	1.6×10^{-5}
30UN2	2.6	9.45	2.6	9.4	10.1	19.5	0.93	1.5×10^{-7}	4.7×10^{-5}
20UN5	—	—	2.9	3.6	1.6	5.2	2.25	2.7×10^{-7}	1.5×10^{-6}
12UN5	—	—	3.7	11.0	6.8	17.8	1.62	1.3×10^{-6}	9.4×10^{-6}

Table 2: Results: $t_{\text{crossover}}$ is the time (if applicable) at which $M_{\text{core}} = M_{\text{env}}$, $M_{\text{crossover}}$ is M_{core} at that time, t_{end} is the time at which the simulation stops, $M_{\text{core,end}}$, $M_{\text{env,end}}$ and $M_{\text{tot,end}}$ correspond to the core, envelope, and total mass at the end of the run, respectively. $f_{\text{solid-to-gas}}$ is the solid-to-gas ratio, $\dot{M}_{\text{core,end}}$ and $\dot{M}_{\text{env,end}}$ are the core accretion rate and the gas accretion rate at the end of the simulation.

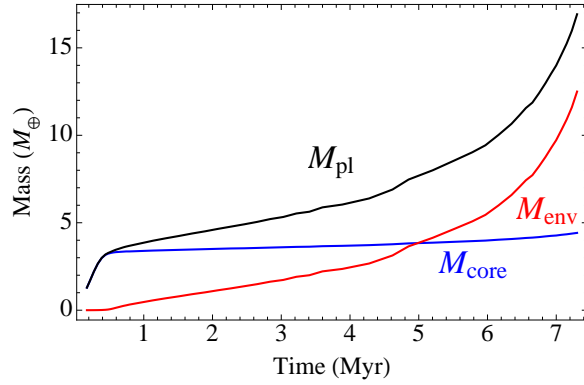
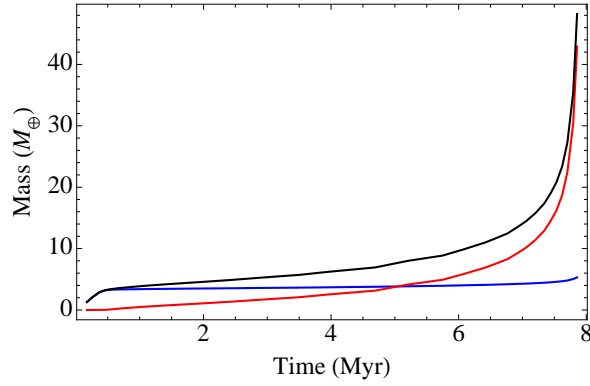
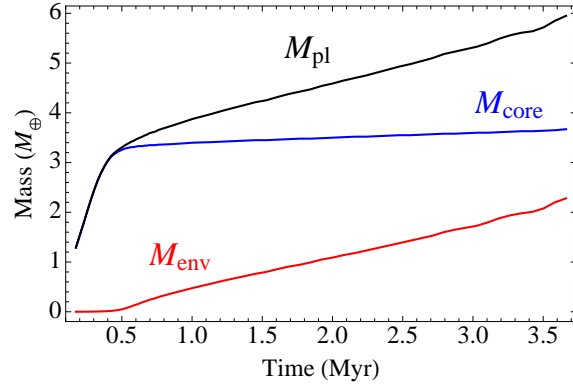


Fig. 1.— Run 20UN1: planetary growth at 20 AU with solid surface density $\sigma_s=0.35 \text{ g cm}^{-2}$ and high accretion rate - $[dM/dt]_{HIGH}$ (Eq. 2). The planetesimal size is 1 km. The red, blue, and black curves represent the mass of the gaseous envelope (hydrogen and helium), core (heavy elements), and total planetary mass, respectively. **Top:** planetary growth up to 3.7 Myr. **Middle:** planetary growth up to 8 Myr. **Bottom:** planetary growth up to ≈ 7.2 Myr, at which time the total mass is $17 M_{\oplus}$.

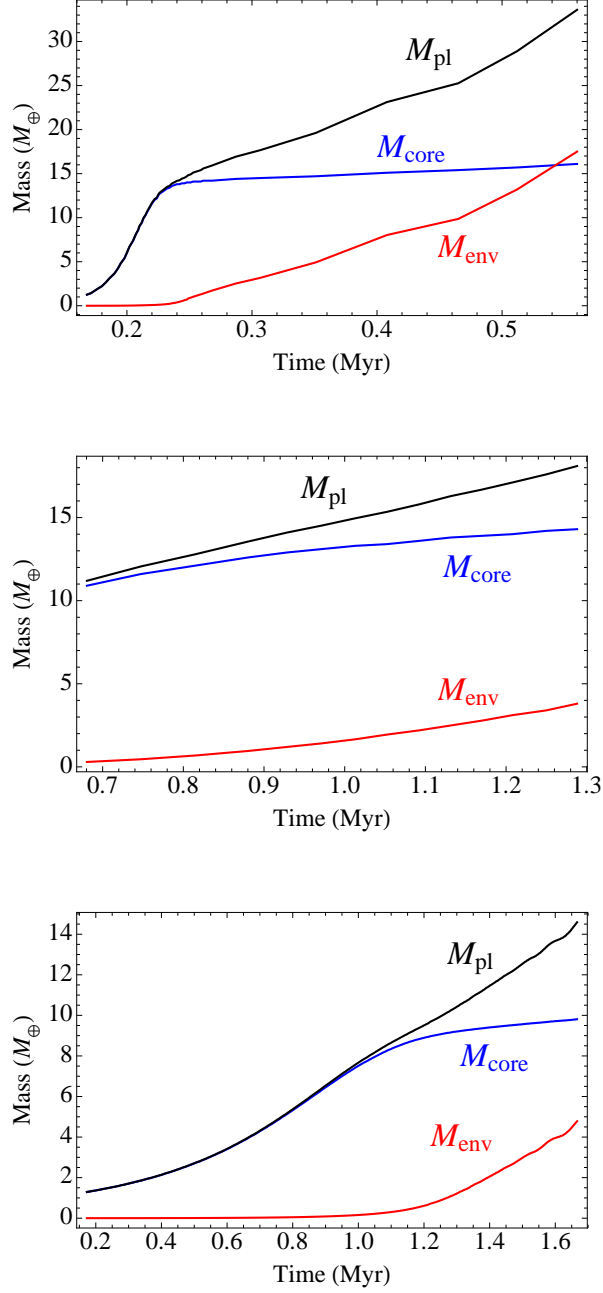


Fig. 2.— Planetary growth at 20 AU, . **Top:** Same as Fig. 1 but with $\sigma_s=3.5 \text{ g cm}^{-2}$ (Run 20UN2). **Middle:** Simulation without planetesimal scattering or envelope enhancement of the core accretion cross section, with $\sigma_s=0.7 \text{ g cm}^{-2}$ and with the high core accretion rate $[dM/dt]_{HIGH}$, Eq. (2) (Run 20UN3). **Bottom:** Simulation with $\sigma_s=1.7 \text{ g cm}^{-2}$ including planetesimal scattering and envelope enhancement of the cross section with 1 km-sized planetesimals. The core accretion rate is taken from Eq. (5), i.e., the transitional accretion rate (Run 20UN4).

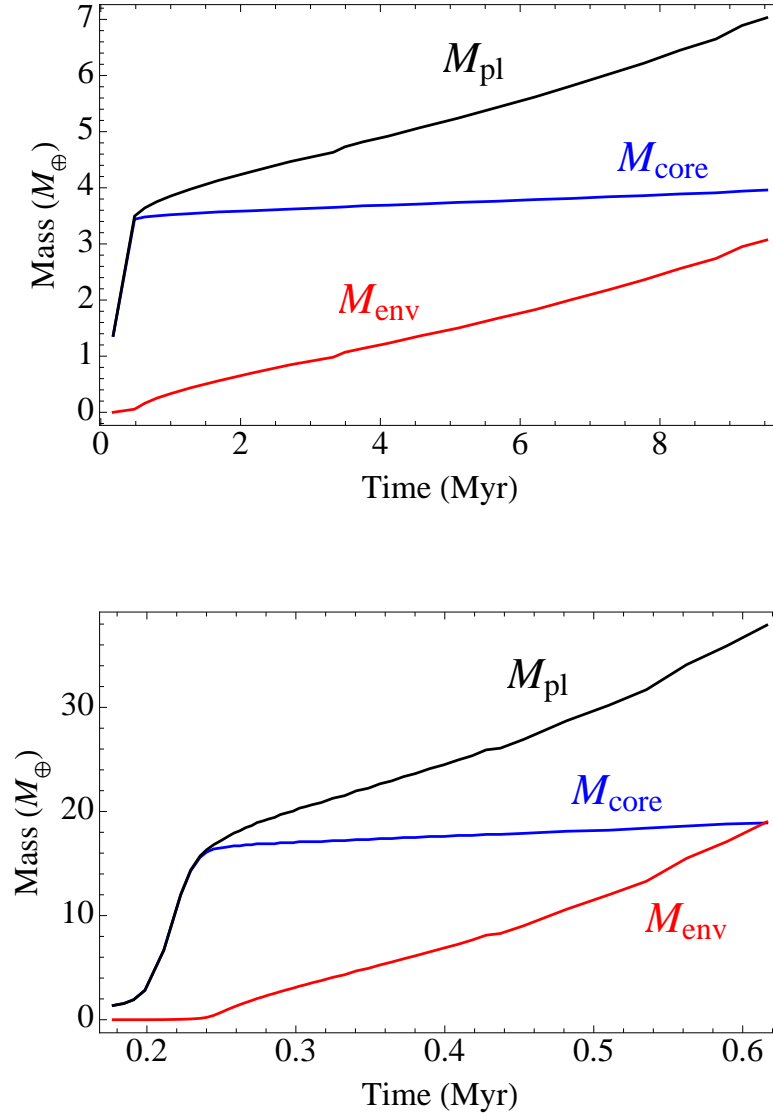


Fig. 3.— **Top:** Run 15UN1— planetary growth at 15 AU with $\sigma_s=0.55 \text{ g cm}^{-2}$ and accretion rate $[\text{dM}/\text{dt}]_{\text{HIGH}}$ (Eq. 2). **Bottom:** Run 15UN2— planetary growth at 15 AU with $\sigma_s=5.5 \text{ g cm}^{-2}$ and accretion rate - $[\text{dM}/\text{dt}]_{\text{HIGH}}$ (Eq. 2).

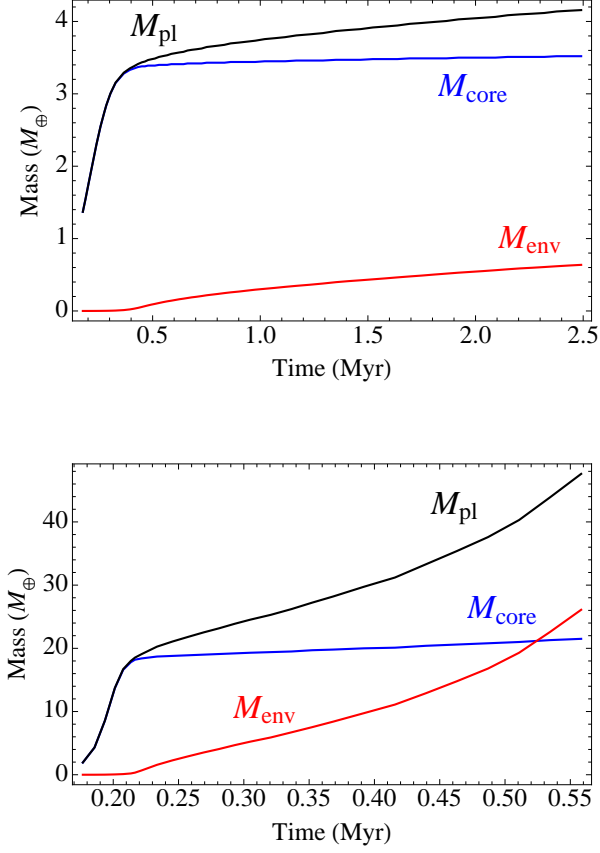


Fig. 4.— **Top:** Run 12UN1— Planetary growth at 12 AU with $\sigma_s=0.75 \text{ g cm}^{-2}$ and the high accretion rate $[dM/dt]_{HIGH}$ (Eq. 2). The planetesimal size is 1 km. The red, blue, and black curves represent the mass of the gaseous envelope (mostly hydrogen and helium), core (heavy elements), and total planetary mass, respectively. **Bottom:** Run 12UN2— planetary growth at 12 AU with $\sigma_s=7.5 \text{ g cm}^{-2}$ and $[dM/dt]_{HIGH}$ (Eq. 2).

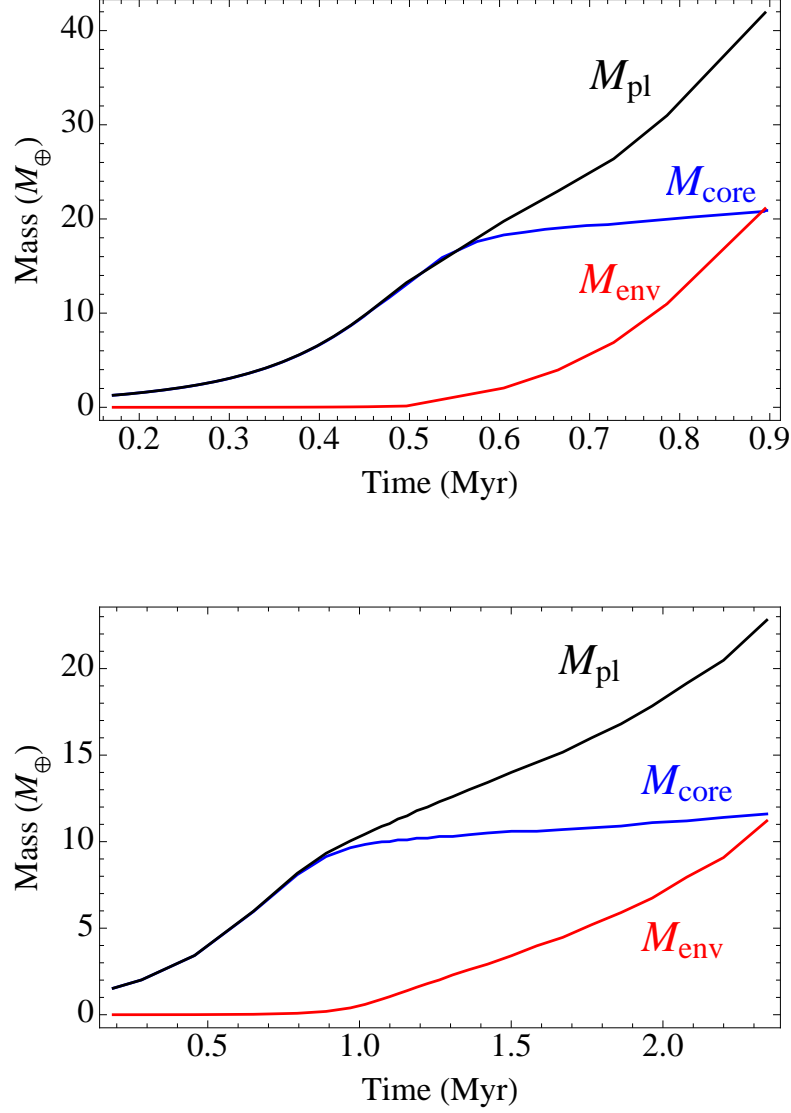


Fig. 5.— **Top:** Run 20UN3—planetary growth at 12 AU with $\sigma_s=7.5 \text{ g cm}^{-2}$ and the transitional accretion rate $[\text{d}M/\text{d}t]_{\text{LOW}}$ (Eq. 5). **Bottom:** Run 20UN4—planetary growth at 12 AU with $\sigma_s=3 \text{ g cm}^{-2}$ and the transitional accretion rate $[\text{d}M/\text{d}t]_{\text{LOW}}$ (Eq. 5).

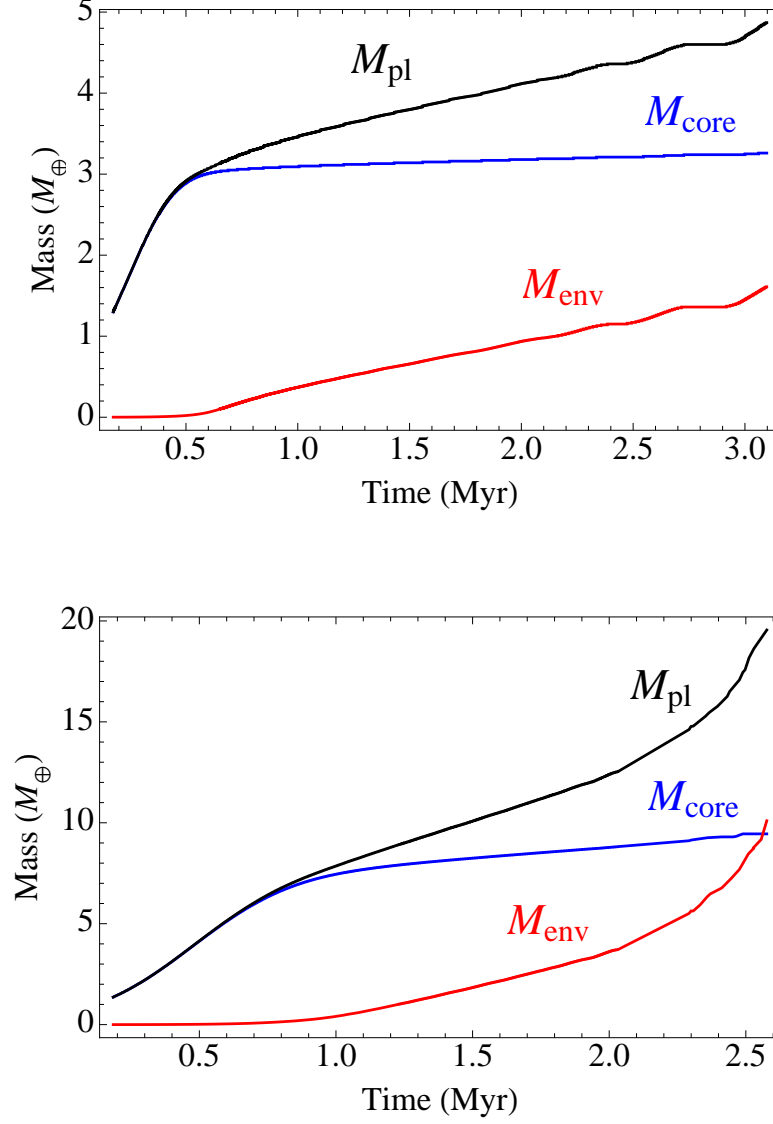


Fig. 6.— **Top:** Run 30UN1– Planet formation at 30 AU assuming $\sigma_s=0.2 \text{ g cm}^{-2}$ and $[dM/dt]_{HIGH}$ (Eq. 2). **Bottom:** Run 30UN2–Same as top panel but without planetesimal scattering.

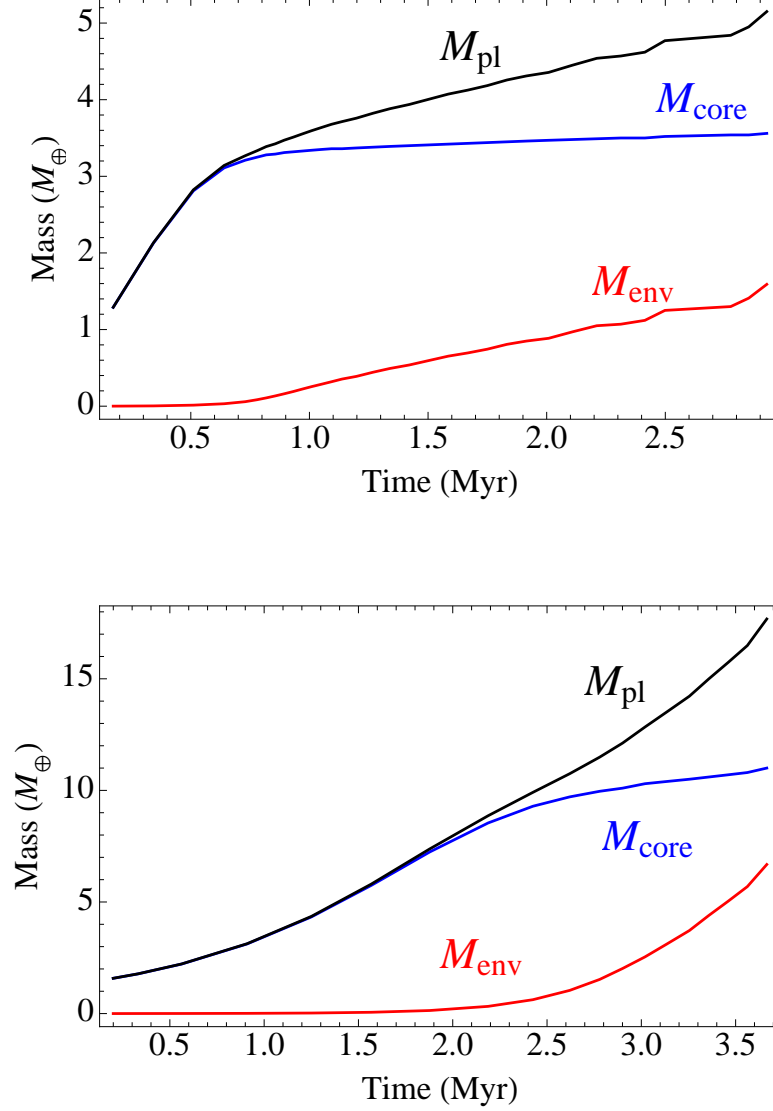


Fig. 7.— Planetary growth with 100 km-sized planetesimals. **Top:** Run 20UN5— planetary formation at 20 AU, $\sigma_s=0.35 \text{ g cm}^{-2}$ with core accretion rate $[\text{dM}/\text{dt}]_{\text{HIGH}}$, i.e. Eq. (2). **Bottom:** Run 12UN5— planetary formation at 12 AU with $\sigma_s=3 \text{ g cm}^{-2}$ and the low core accretion rate $[\text{dM}/\text{dt}]_{\text{LOW}}$ (Eq. 5).